



A Local Multi-grid X-FEM approach applied to crack growth simulations

**Anthony Gravouil
Johann Rannou
Marie-Christine Baietto**

LAMCOS / INSA de LYON / CNRS UMR 5259 / FRANCE

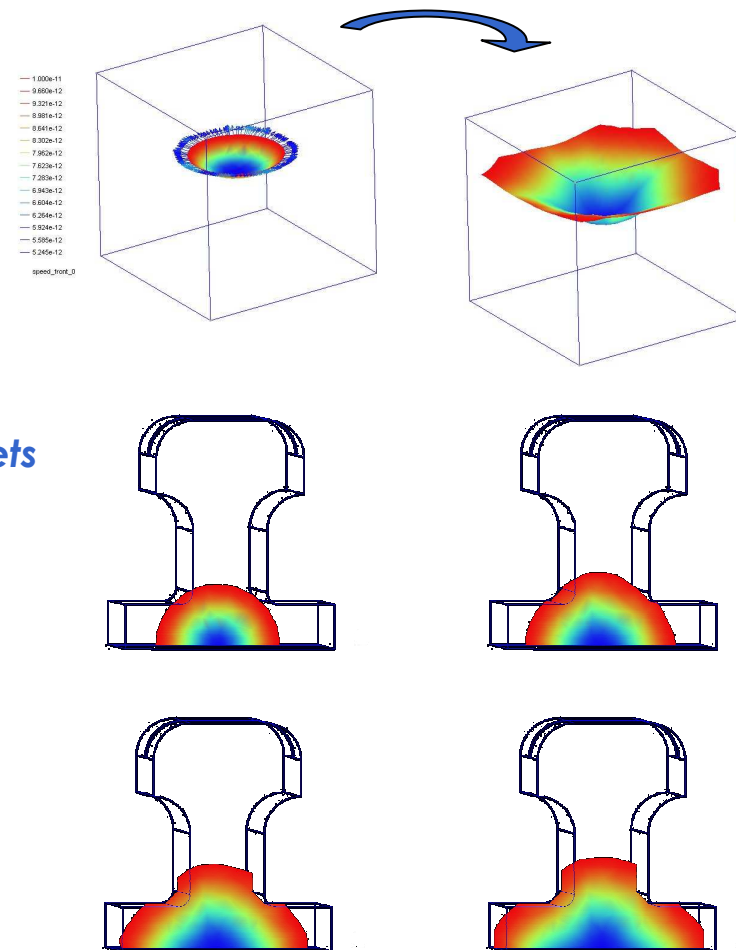
anthony.gravouil@insa-lyon.fr

OUTLINE

- 1 *Introduction of X-FEM+level sets for crack modeling*
- 2 *An example of multi-scale approach coupled with X-FEM*
- 3 *Conclusions & perspectives*

Introduction

- **eXtended Finite Element Method + level sets**
- **Advantages:**
 - *Similar to FEM*
 - *No remeshing*
 - *No field interpolation*
 - *Good topologic properties*
 - *Flexibility in the initialization of level sets*
- **Drawbacks:**
 - *Specific numerical integration and preconditioning*
 - *Post-treatment*
 - *Specific strategies of enrichment for time-dependent problems*

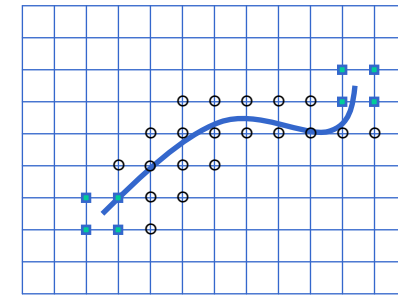


Introduction

- **Local partition of unity (two scale strategy):**

- **Discontinuous and asymptotic enrichment of the displacement field**

$$\begin{aligned}
 \mathbf{U}_x &= \sum_{\mathbf{N}} \mathbf{N}_x \mathbf{u} + \sum_{\mathbf{H}} \mathbf{N}_x \mathbf{H} \\
 \mathbf{F} &= \left\{ \sqrt{\frac{\rho}{2}} \begin{pmatrix} 0 \\ -2 \end{pmatrix}, \sqrt{\frac{\rho}{2}} \begin{pmatrix} 0 \\ -2 \end{pmatrix}, \sqrt{\frac{\rho}{2}} \begin{pmatrix} 0 \\ -2 \end{pmatrix}, \dots, \sqrt{\frac{\rho}{2}} \begin{pmatrix} 0 \\ -2 \end{pmatrix} \right\}
 \end{aligned}$$



- **Crack shape modeling by two level sets:**

$$\begin{aligned}
 \begin{pmatrix} \cdot \\ \cdot \\ \cdot \end{pmatrix} & \cdot \begin{pmatrix} \cdot \\ \cdot \\ \cdot \end{pmatrix} & \cdot & \text{crack} \\
 \begin{pmatrix} \cdot \\ \cdot \\ \cdot \end{pmatrix} & \cdot \begin{pmatrix} \cdot \\ \cdot \\ \cdot \end{pmatrix} & \cdot & \text{Crack front} \\
 \begin{pmatrix} \cdot \\ \cdot \\ \cdot \end{pmatrix} & \cdot \begin{pmatrix} \cdot \\ \cdot \\ \cdot \end{pmatrix} & \cdot & \text{Crack virtual extension}
 \end{aligned}$$

Local orthogonality

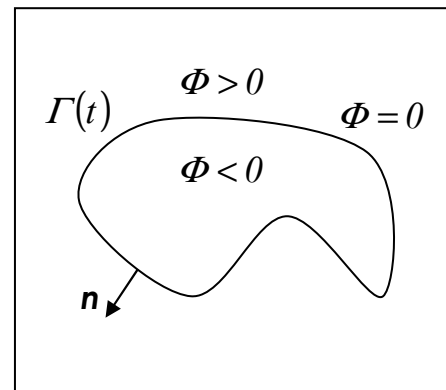
- **Level set update**

$$\frac{\partial \phi}{\partial t} + \mathbf{V} \cdot \nabla \phi = 0$$

[Moës 1999, Stolarska 2001, Dufloot 2005, Béchet 2005, Sukumar 2007] [Sethian 1997]

[Gravouil A., Moës N., Belytschko T., IJNME, 2002]

Level sets



Signed distance:

$$\begin{cases} \Phi(\mathbf{x}, t) < 0 & \text{in } \Omega^-(t) \\ \Phi(\mathbf{x}, t) = 0 & \text{on } \Gamma(t) \\ \Phi(\mathbf{x}, t) > 0 & \text{in } \Omega^+(t) \end{cases}$$

➡ Allows to model implicitly moving interfaces

- **Governing equation:** $\frac{\partial \Phi}{\partial t} + V|\nabla \Phi| = 0$

- **Normal vector:** $\mathbf{n} = \frac{\nabla \Phi}{|\nabla \Phi|}$ **curvature:** $\kappa = \nabla \cdot \frac{\nabla \Phi}{|\nabla \Phi|}$

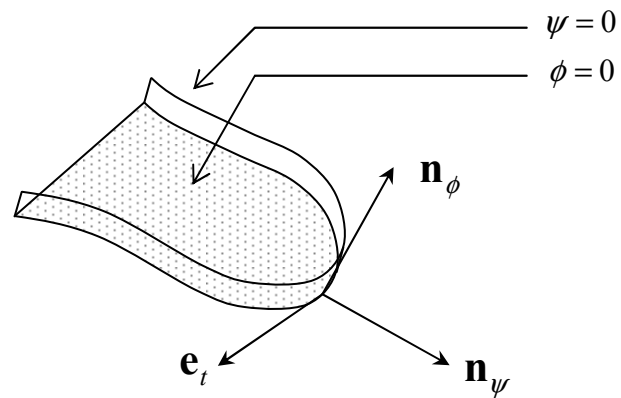
- **Hausdorff measure:** $|\Gamma(t)| = \int \delta(\Phi) |\nabla \Phi| dx$

[Osher and Sethian 1988]

- **Lebesgue measure:** $|\Omega^-(t)| = \int H(-\Phi) dx$

Non-planar crack modeling

- Local basis linked to the level sets



$$\mathbf{n}_\psi = \nabla \psi$$

$$\mathbf{n}_\phi = \nabla \phi$$

$$\mathbf{e}_t = \mathbf{n}_\psi \times \mathbf{n}_\phi$$

- Component velocity on the local basis of the crack front V_ϕ and V_ψ

$$\mathbf{V} = V_\psi \mathbf{n}_\psi + V_\phi \mathbf{n}_\phi$$

Non-planar crack modeling

- **Initialization and re-initialization** $|\nabla \psi| = 1$ $\frac{\partial \psi}{\partial \tau} + \text{sign}(\psi)(|\nabla \psi| - 1) = 0$

- **Extension of the velocity field** $\nabla \phi \cdot \nabla V_\phi = 0$ [Peng and al. 1999]

$$\frac{\partial V_\phi}{\partial \tau} + \text{sign}(\phi) \frac{\nabla \phi}{|\nabla \phi|} \cdot \nabla V_\phi = 0$$

$$\frac{\partial V_\phi}{\partial \tau} + \text{sign}(\psi) \frac{\nabla \psi}{|\nabla \psi|} \cdot \nabla V_\phi = 0$$

$$\mathbf{n}_\psi \cdot \nabla V_\phi = 0$$

$$\mathbf{n}_\phi \cdot \nabla V_\phi = 0$$

- **Update of the level sets** $\frac{\partial \phi}{\partial t} + V_\phi |\nabla \phi| = 0$ $\frac{\partial \psi}{\partial t} + V_\psi |\nabla \psi| = 0$

- **Re-orthogonalization:**

$$\frac{\partial \psi}{\partial \tau} + \text{sign}(\phi) \frac{\nabla \phi}{|\nabla \phi|} \cdot \nabla \psi = 0$$



$$\nabla \phi \cdot \nabla \psi = 0$$

Non-planar crack modeling

- **Time and space discretization for structured meshes**

$$\phi_{ij}^{n+1} = \phi_{ij}^n - \Delta t \left\{ \begin{array}{l} (s_{ij} n_{ij}^x)^+ \frac{\phi_{ij} - \phi_{i-1j}}{\Delta x} + (s_{ij} n_{ij}^x)^- \frac{\phi_{i+1j} - \phi_{ij}}{\Delta x} \\ + (s_{ij} n_{ij}^y)^+ \frac{\phi_{ij} - \phi_{ij-1}}{\Delta y} + (s_{ij} n_{ij}^y)^- \frac{\phi_{ij+1} - \phi_{ij}}{\Delta y} \end{array} \right\}$$

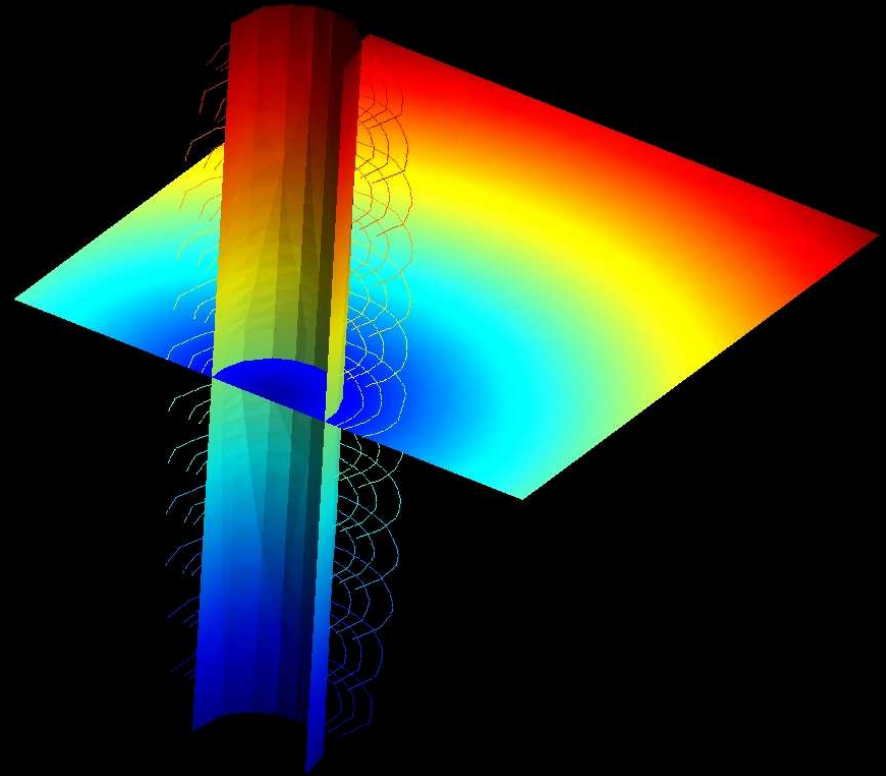
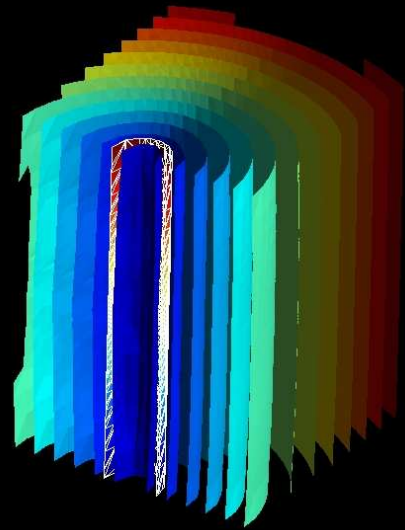
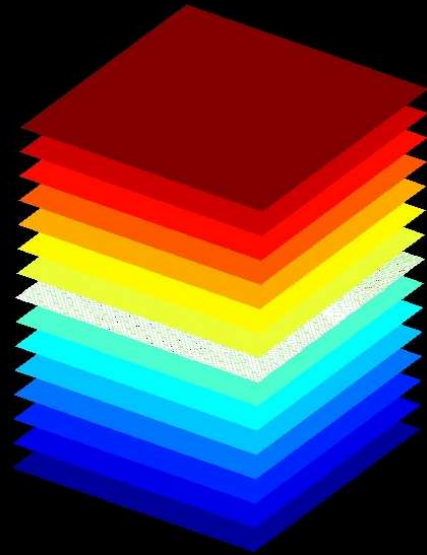
$$\left\{ \begin{array}{l} \tilde{\Phi}^{n+1} = \Phi^n - \Delta t H(\Phi^n) \\ \Phi^{n+1} = \frac{(\Phi^n + \tilde{\Phi}^{n+1})}{2} - \frac{\Delta t}{2} H(\tilde{\Phi}^{n+1}) \end{array} \right.$$

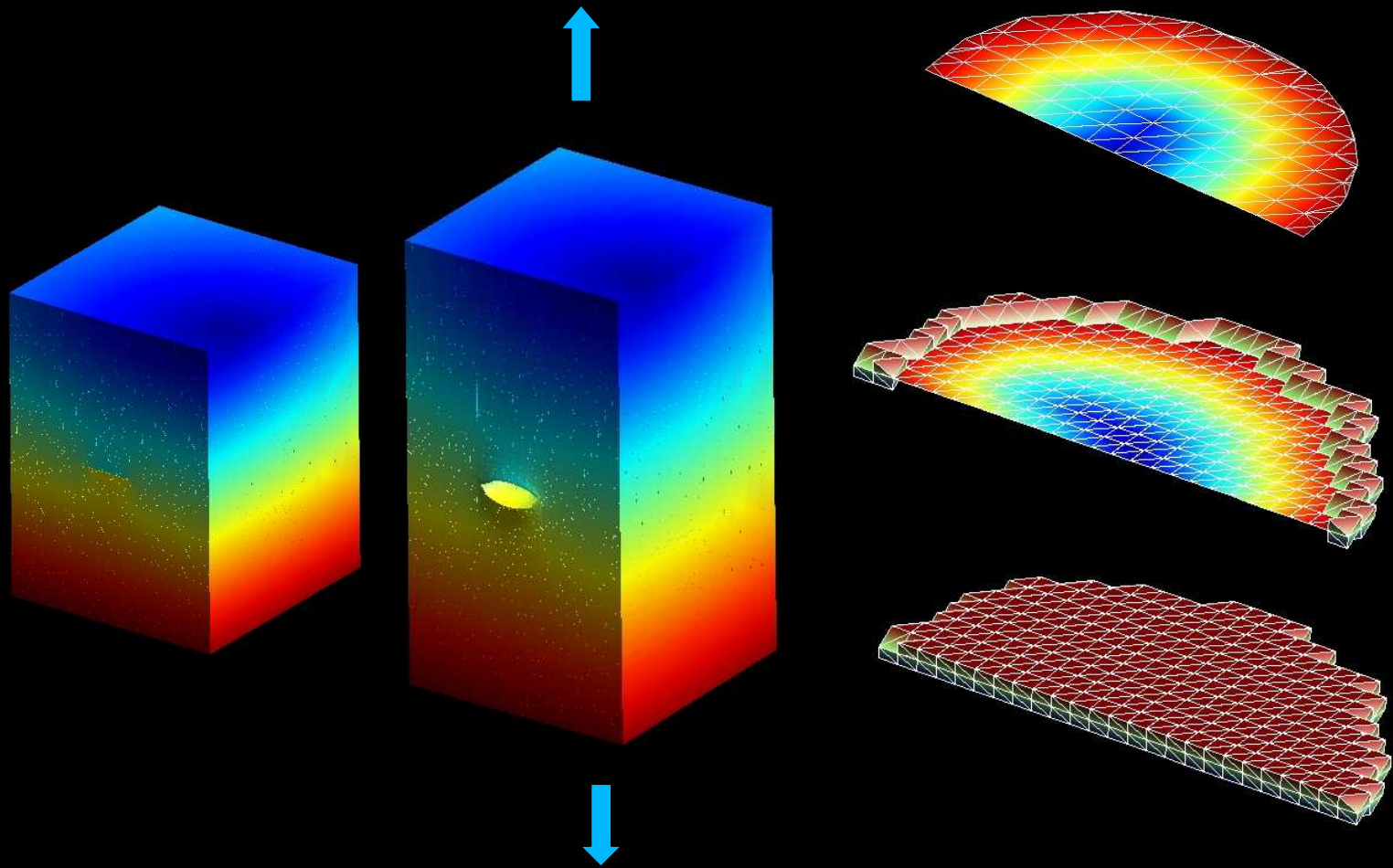
$$(x)^+ = \max(x, 0) \quad (x)^- = \min(x, 0) \quad s_{ij} = \frac{\Phi_{ij}}{\sqrt{\Phi_{ij}^2 + \Delta x^2}}$$

- **Time and space discretization for non-structured meshes**

$$\left\{ \begin{array}{l} \frac{\partial \phi}{\partial t} + H(\nabla \phi, \mathbf{x}, t) = 0 \\ \phi(\mathbf{x}, 0) = \phi_0(\mathbf{x}) \end{array} \right. \quad \begin{array}{l} \text{Space: [Barth and Sethian 1998]} \\ \text{Time: Runge Kutta} \end{array}$$

⇒ **Numerical schemes stable, accurate and convergent.
However, finite difference approaches are more accurate
for an equivalent size element mesh**





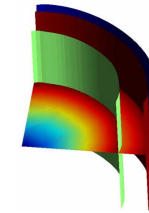
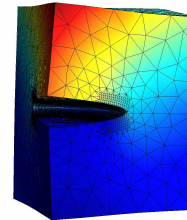
ELFE_3D

GMSH

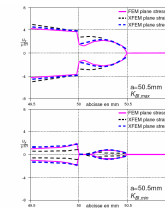
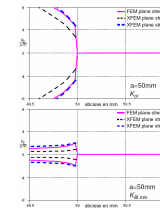
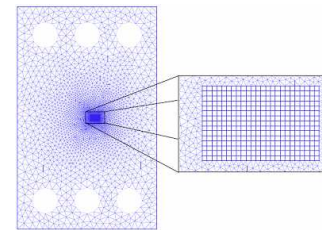
Scale effects and numerical discretization:

- Some previous works show that we need to « capture » the following length scales:

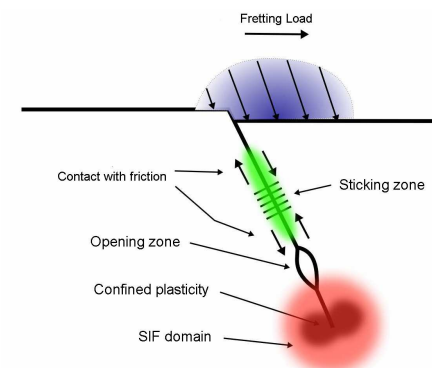
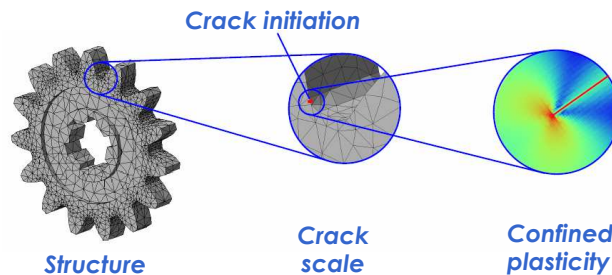
- Area influenced by the asymptotic behavior close to the crack front



- Confined plasticity, closure effect



- Localized non-linearities due to contact and friction along the crack faces



When several length scales occur, one may question the relevant spatial discretization needed to reach a given accuracy (with enrichment functions)

OUTLINE

- 1 *Introduction of X-FEM+level sets for crack modeling*
- 2 *An example of multi-scale approach coupled with X-FEM*
- 3 *Conclusions & perspectives*

Multi-scale strategies coupled with X-FEM

- Agreement between the discretization of the structure and the geometric modeling of the crack (in presence of enrichments) ?
- Agreement between the discretization of the structure and the area influenced by the crack front singularity (in presence of enrichments) ?
- Agreement between the discretization of the structure and local non-linearities on the crack faces or / and in the bulk (in presence of enrichments) ?
- Which kind of strategy of enrichment to consider (topologic enrichment, geometric enrichment, enrichment of all scales) ?

➡ Different numerical multi-scale strategies:

- Multi-grid strategies
- Micro-macro approaches
- Partition of unity
- ...

[Guidault P.-A., Allix O., Champaney L., Cornuault B., 2007] [Allix O., 2006] [Ladevèze O., Loiseau O., Dureisseix D., 2001]

[Chinesta & al. 2007] [Fish J., Yuan Z., 2005] [Ben Dhia H., Rateau G., 2005] [Qian D., Wagner G., Liu W., 2004] [Feyel F., 2003]

[Venner C., Lubrecht A., 2000] [Fish J., Pandheeradi M., Belsky V., 1995] [Parsons I., Hall J., 1990] [Brandt A., 1977]

Multi-grid methods

- *Fluid mechanics [Brandt 1977] [Hackbush et Trottenberg 1981] [Hackbush 1985]*
- *Application to linear solid mechanics [Parsons et Hall 1990]*
Application to non-linear solid mechanics [Kacou et Parsons 1993]

$$\mathbf{U} \equiv \mathbf{P}\bar{\mathbf{U}} + \mathbf{U}_f = \mathbf{U}_g + \mathbf{U}_f$$

- ① *first relaxation step (smoothing)*

$$\mathbf{U}^k \rightarrow \tilde{\mathbf{U}}^k = \mathbf{U}^k + \Delta\mathbf{U}_f^{k+1/2} \quad \text{and} \quad \tilde{\mathbf{R}}^k$$

- ② *restriction of the residual on the coarse scale*

$$\bar{\mathbf{R}}^k = \mathbf{P}^T \tilde{\mathbf{R}}^k$$

- ③ *direct solving on the coarse scale (recursive for more than 2 grids)*

$$\bar{\mathbf{K}}\Delta\bar{\mathbf{U}}^{k+1} = \bar{\mathbf{R}}^k$$

- ④ *prolongation of the displacement on the fine scale*

$$\Delta\mathbf{U}_g^{k+1} = \mathbf{P}\Delta\bar{\mathbf{U}}^{k+1}$$

- ⑤ *correction*

$$\mathbf{U}^{k+1/2} = \tilde{\mathbf{U}}^k + \Delta\mathbf{U}_g^{k+1} \quad \text{and} \quad \mathbf{R}^{k+1}$$

- ⑥ *last relaxation step*

$$\mathbf{U}^{k+1/2} \rightarrow \mathbf{U}^{k+1}$$

Different definitions of the prolongation operator

- *Nodal definition (collocation method)*

$$\mathbf{u}^f(\mathbf{x}_n) = \mathbf{u}^c(\mathbf{x}_n)$$

$$\mathbf{u}_n^f + \mathbf{a}_n^f H(\mathbf{x}_n) + \sum_{j=1}^4 \mathbf{b}_{jn}^f \gamma_j(\mathbf{x}_n) = \mathbf{u}^c(\mathbf{x}_n)$$

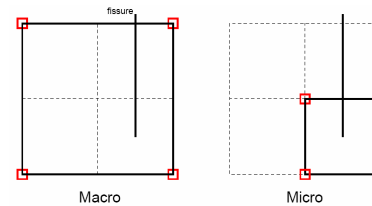
- *Variational definition (mortar method)
(unambiguously definition of the coefficients)*

$$\int_{\Omega} \mathbf{u}^f(\mathbf{x}) \mathbf{u}^{f*}(\mathbf{x}) d\Omega = \int_{\Omega} \mathbf{u}^c(\mathbf{x}) \mathbf{u}^{f*}(\mathbf{x}) d\Omega \quad \forall \mathbf{u}^{f*}$$

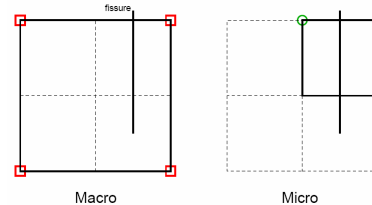
$$\mathbf{M}_{ff} \mathbf{U}_f = \mathbf{M}_{fc} \mathbf{U}_c \quad \Rightarrow \quad \mathbf{P} = \mathbf{M}_{ff}^{-1} \mathbf{M}_{fc}$$

An example of multi-scale strategy coupled with X-FEM A nodal approach for the prolongation operator definition

- **Compatible enrichment**



- **Incompatible enrichment**



➡ **One interpolates separately standard fields and enriched fields (in both cases)**

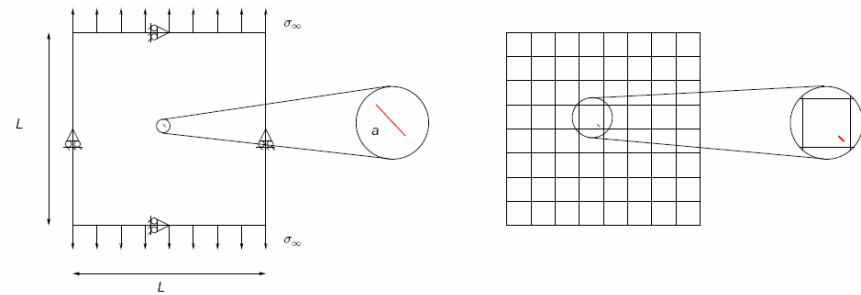
- $$\vec{U}^g(\vec{x}) = \sum_{i \in \mathcal{N}} N_i^g(\vec{x}) \vec{u}_i^g + \sum_{i \in \mathcal{N}_{sing}} \sum_{j=1}^4 N_i^g(\vec{x}) \gamma_j(\vec{x}) \vec{b}_{ji}^g$$

- $$\vec{U}^f(\vec{x}_i) = \vec{u}_i^f + \vec{a}_i^f H(\vec{x}_i) \quad \text{with} \quad \begin{aligned} \vec{u}_i^f &= \sum_{j \in \mathcal{N}} N_j^g(\vec{x}_i) \vec{u}_j^g \\ \vec{a}_i^f H(\vec{x}_i) &= \sum_{j \in \mathcal{N}_{sing}} \left(N_j^g(\vec{x}_i) \sum_{k=1}^4 \gamma_k(\vec{x}_i) \vec{b}_{jk}^g \right) \end{aligned}$$

➡ **Local error due to prolongation step (high frequency error) immediately captured by relaxation step**

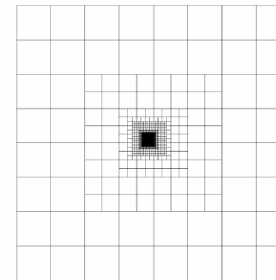
An example of multi-scale strategy coupled with X-FEM

- Crack in a quasi-infinite tensile plate



- Different grids used with the X-L-MG algorithm

9 grids ($h_1/h_9 = 256$)

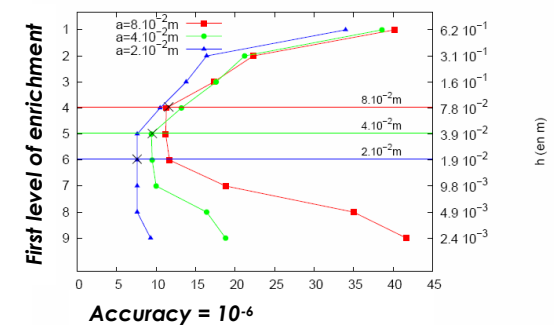


l	$h(m)$	enrichment
1	$6,25 \cdot 10^{-1}$	×
2	$3,12 \cdot 10^{-1}$	×
3	$1,56 \cdot 10^{-1}$	×
4	$7,80 \cdot 10^{-2}$	✓
5	$3,90 \cdot 10^{-2}$	✓
6	$1,95 \cdot 10^{-2}$	✓
7	$9,77 \cdot 10^{-3}$	✓
8	$4,88 \cdot 10^{-3}$	✓
9	$2,44 \cdot 10^{-3}$	✓

Element size (h) of the first enriched grid of the order of the crack length (a)

[Rannou J., Gravouil A., Baietto M.-C, IJNME, 2008]

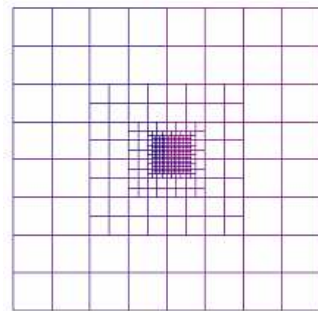
Number of cycles for 3 crack lengths



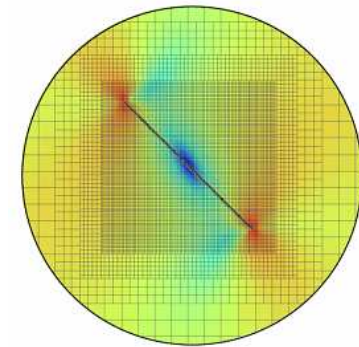
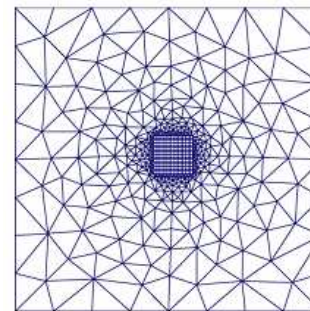
An example of multi-scale strategy coupled with X-FEM

- CPU time for both local multi-grid method and preconditioned conjugate gradient

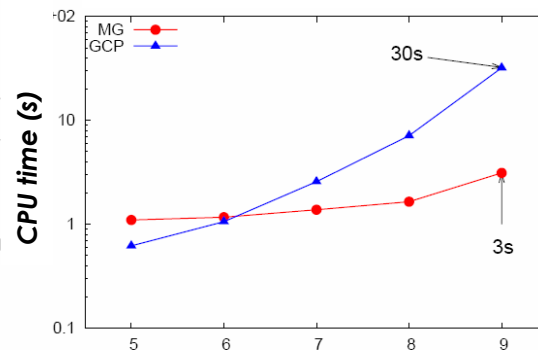
X-L-MG mesh



PCG mesh



CPU time for both methods



MG cycle number	collocation operator	mortar operator
1	$2.09 \cdot 10^{-01}$	$2.10 \cdot 10^{-01}$
2	$4.72 \cdot 10^{-03}$	$4.38 \cdot 10^{-03}$
3	$2.03 \cdot 10^{-04}$	$1.76 \cdot 10^{-04}$
4	$1.53 \cdot 10^{-05}$	$1.33 \cdot 10^{-05}$
5	$1.58 \cdot 10^{-06}$	$1.41 \cdot 10^{-06}$
6	$2.17 \cdot 10^{-07}$	$1.99 \cdot 10^{-07}$
7	$4.09 \cdot 10^{-08}$	$4.56 \cdot 10^{-08}$
8	$6.34 \cdot 10^{-09}$	$6.08 \cdot 10^{-09}$

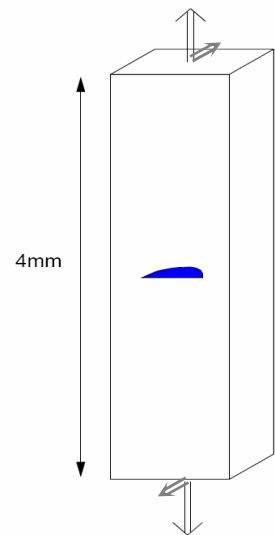
⇒ CPU time lower and complexity with lower order compared to PCG (n versus $n^{1.5}$)

⇒ Similar numerical convergence rate for collocation and mortar operators

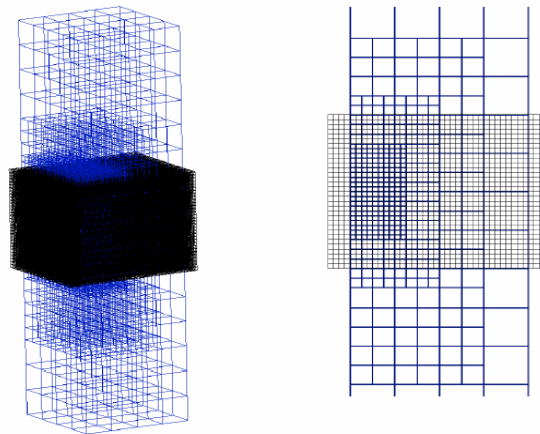
An example of multi-scale strategy coupled with X-FEM

- *Semi-circular crack in a 3D beam submitted to mode I and mixed mode*

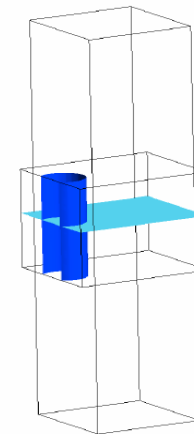
Geometry and B.C.



Structure mesh and level set mesh



Level sets



➡ **The geometrical modeling of the crack is independent of the structure discretization**

[Rannou J., Gravouil A., Baietto M.-C., IJNME, 2008]

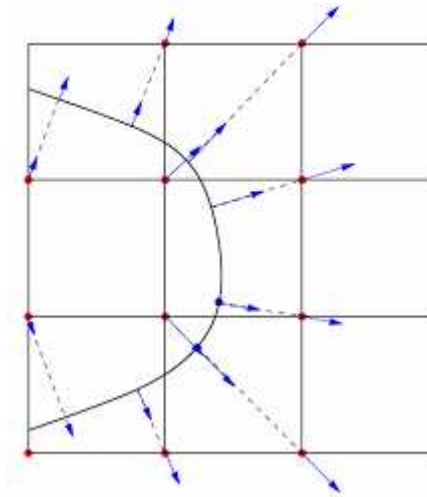
Definition of nodes along the crack front for SIF's calculation

- **Accurate definition of nodes from level sets**

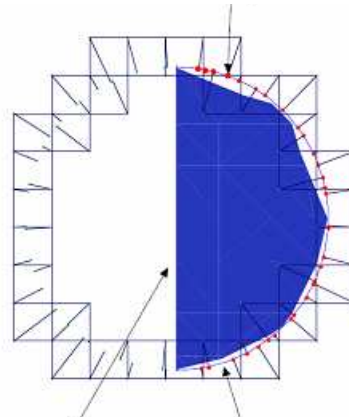
$$\underline{u} = -\psi \nabla \psi - \phi \nabla \phi$$

- **Calculation of Stress Intensity factors on these nodes**

- **Extension of the front velocity to closest mesh nodes (no interpolation)**

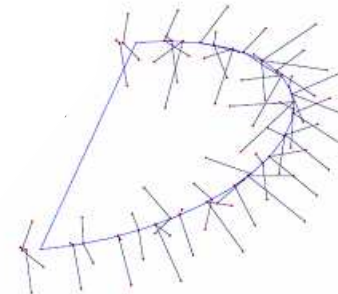


Nodes from gradients of level sets



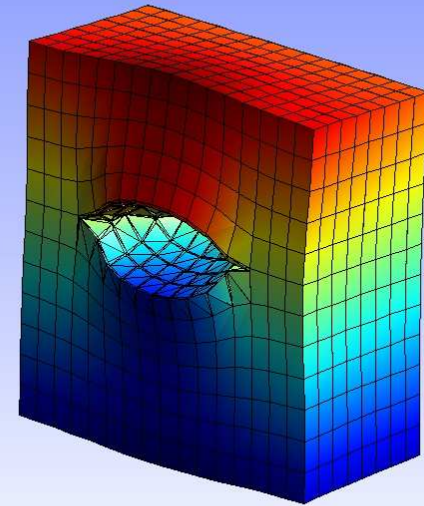
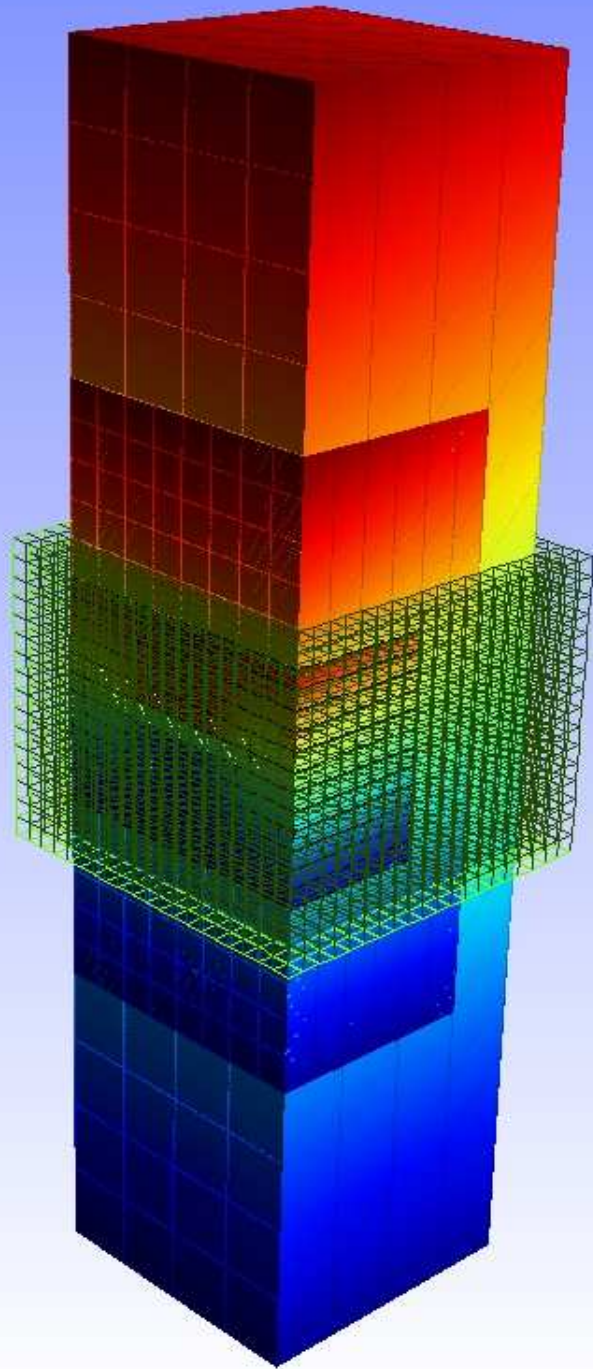
coarse interpolation of the level sets

fine interpolation of the level sets

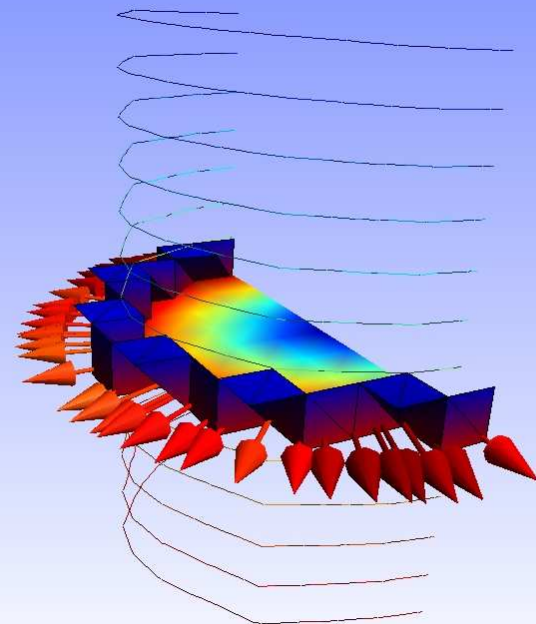


ELFE_3D
GMSH

0

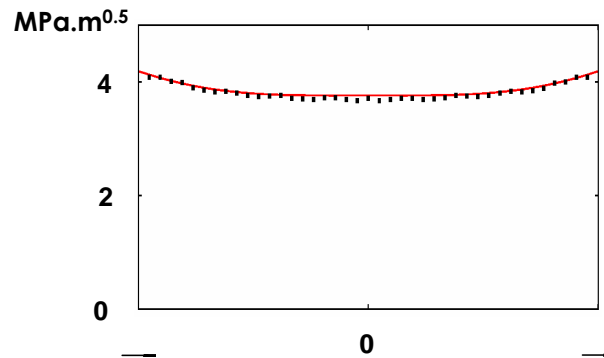


0



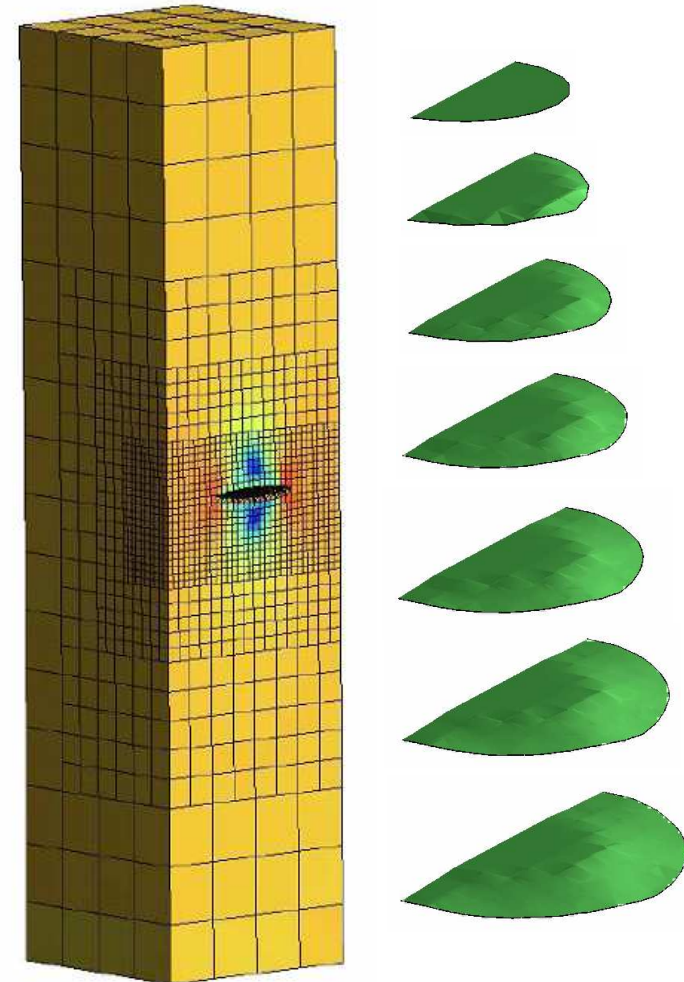
An example of multi-scale strategy coupled with X-FEM

- **Comparison between numerical and analytical K_I in mode I (Raju and Newman)**

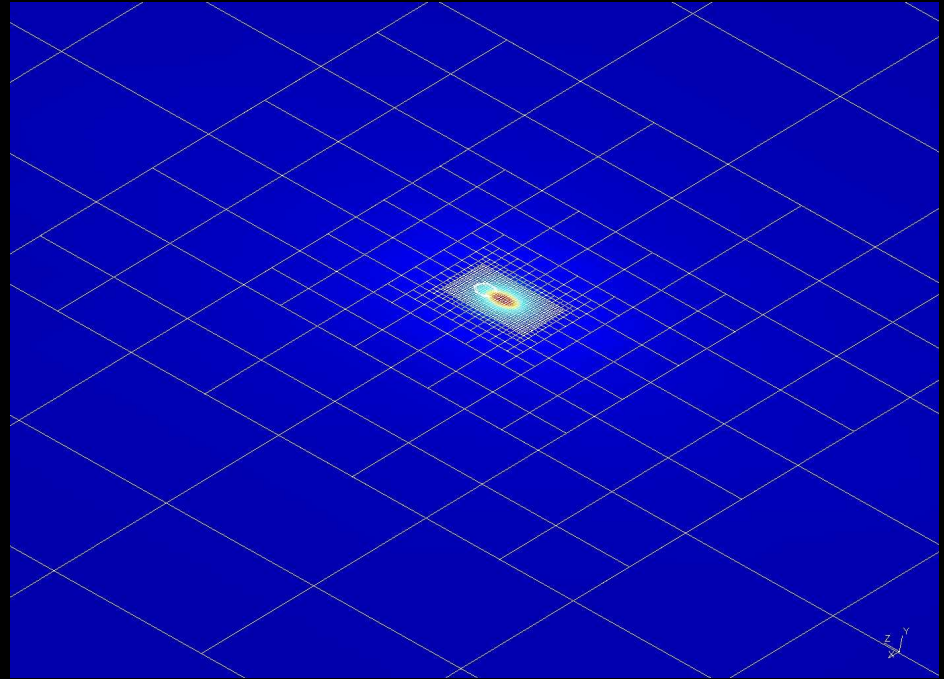
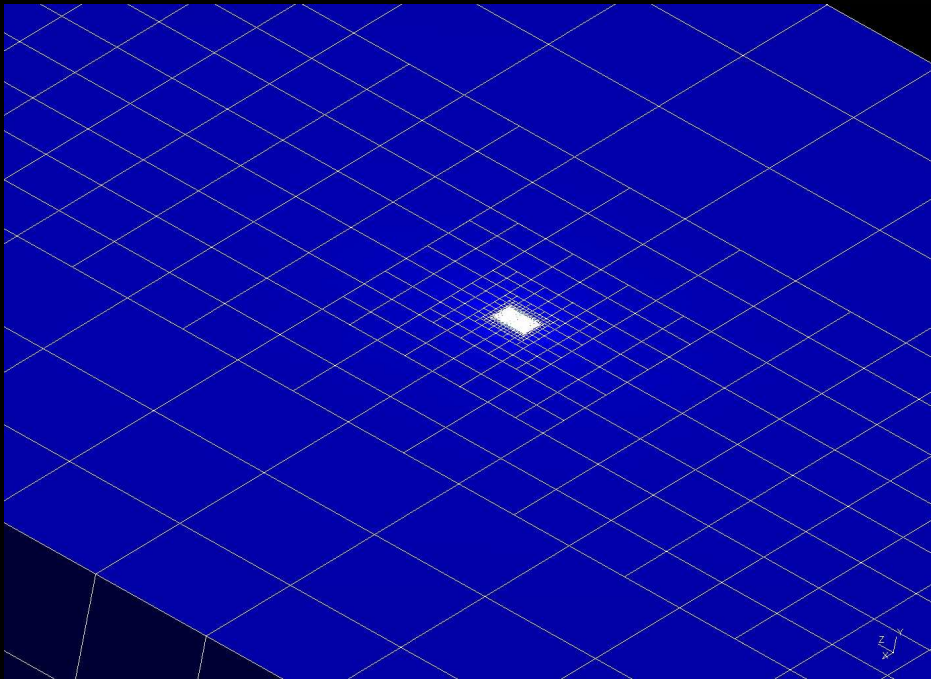
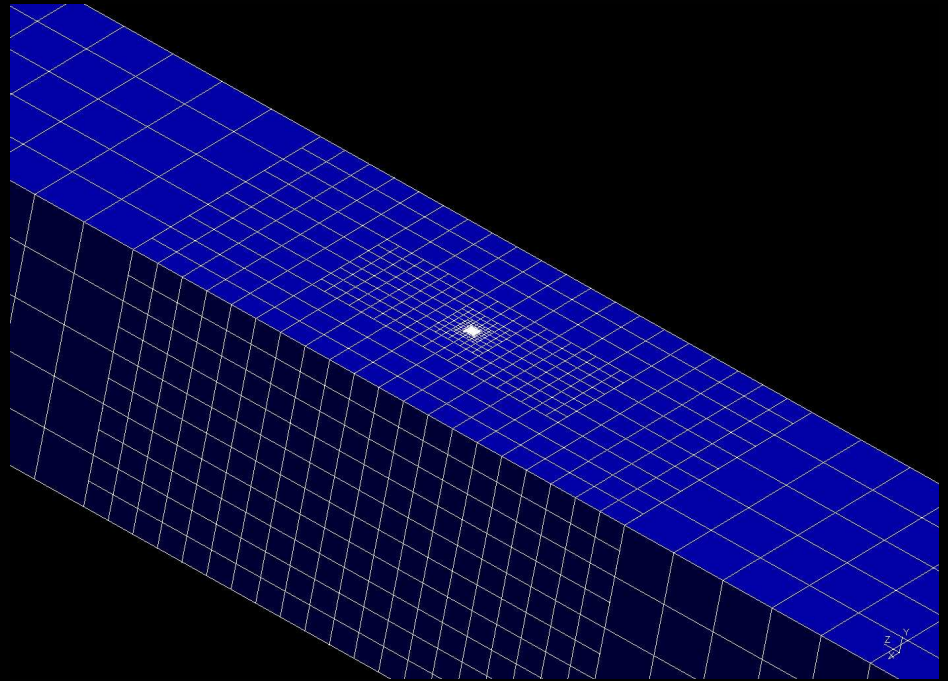
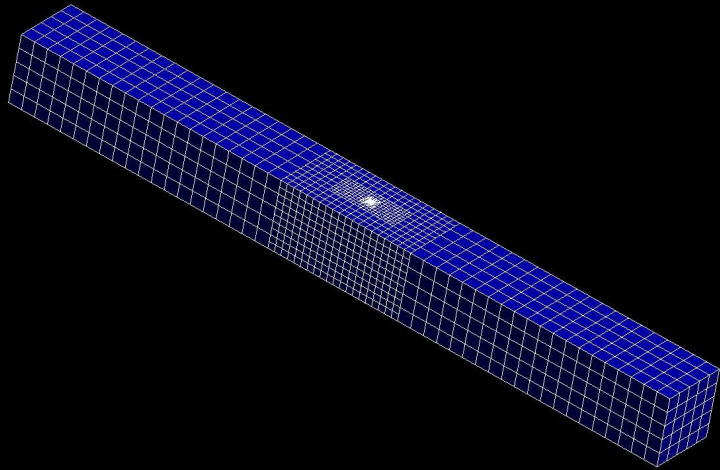


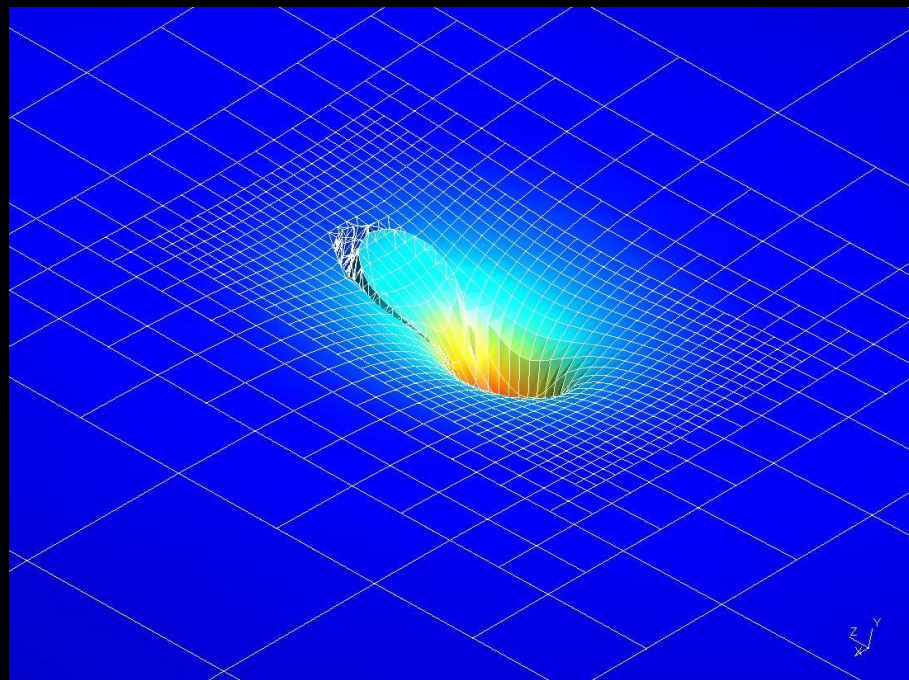
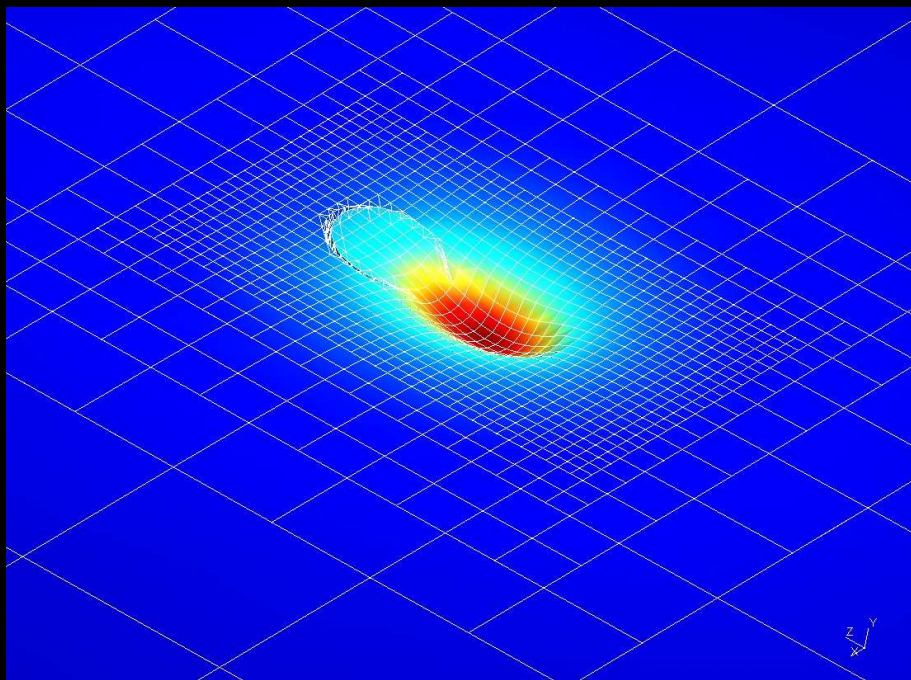
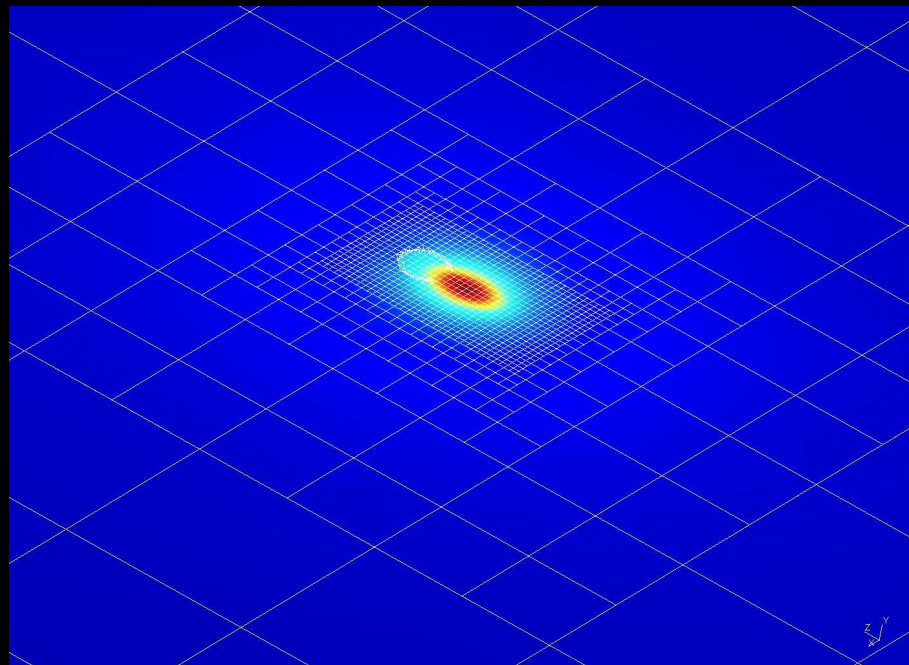
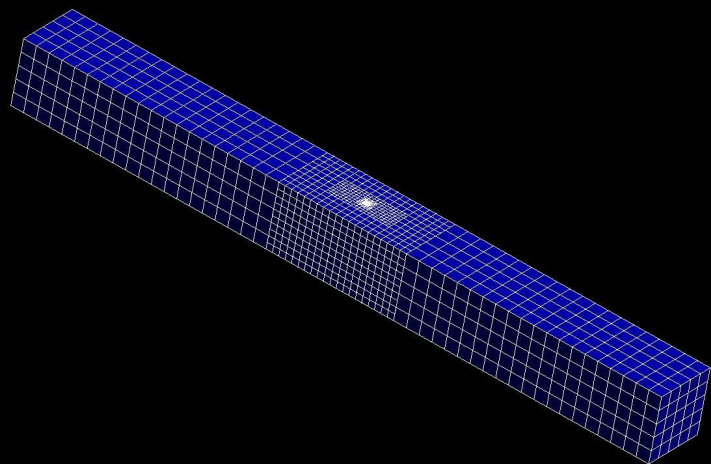
- **Deformed mesh and fatigue crack propagation in mixed mode**

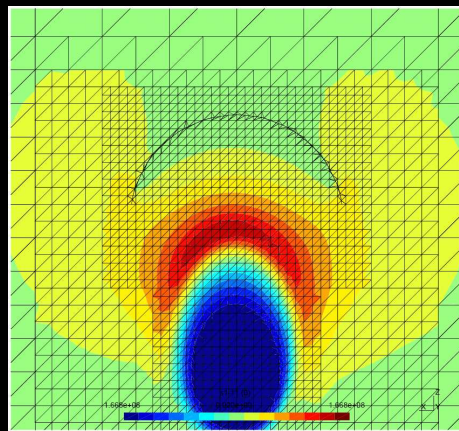
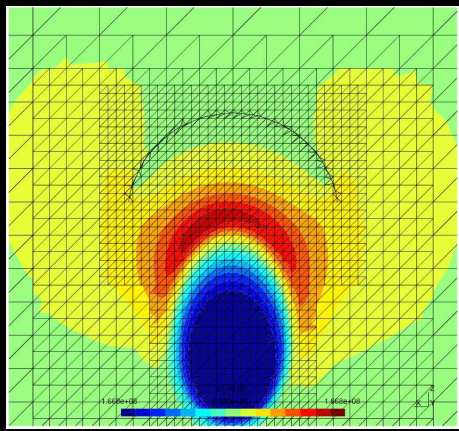
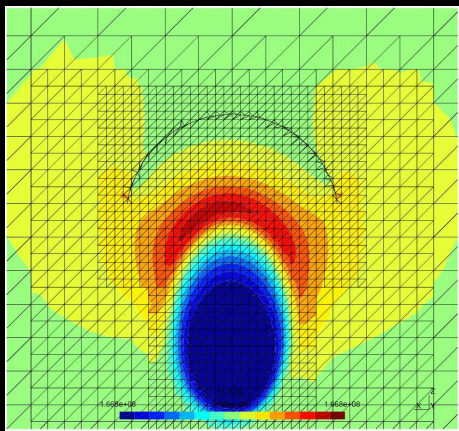
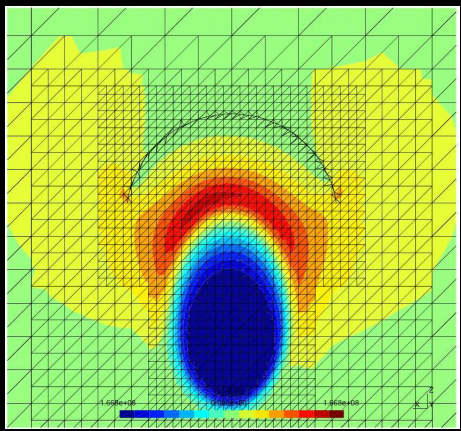
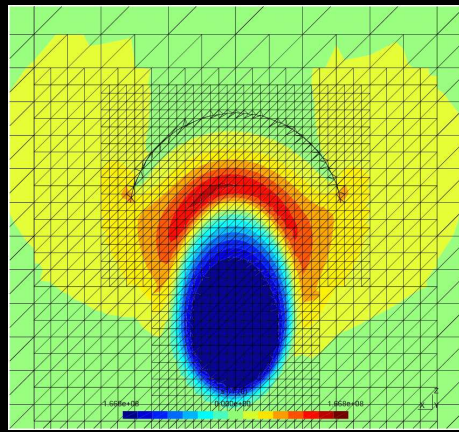
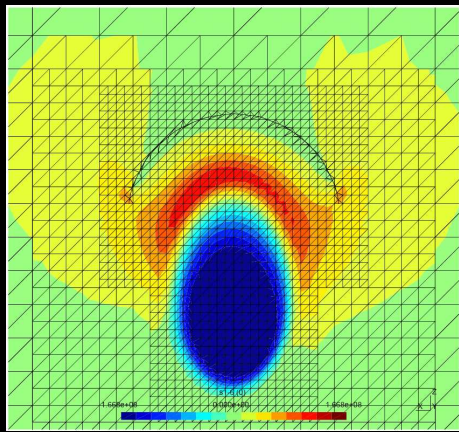
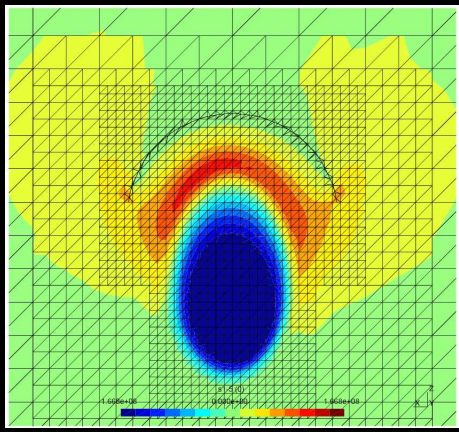
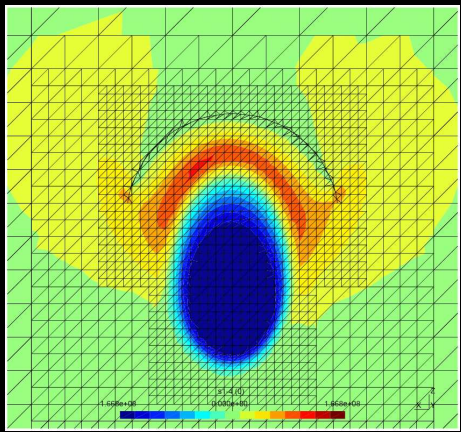
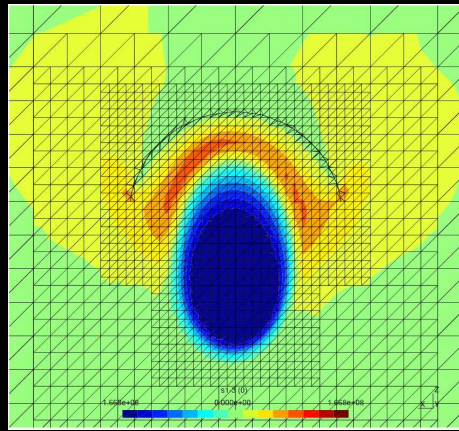
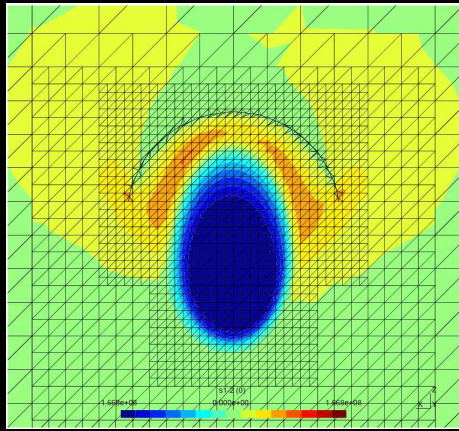
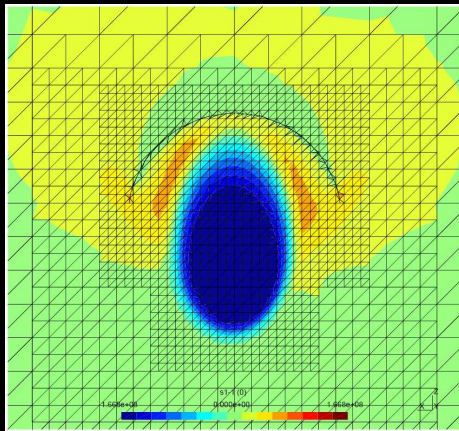
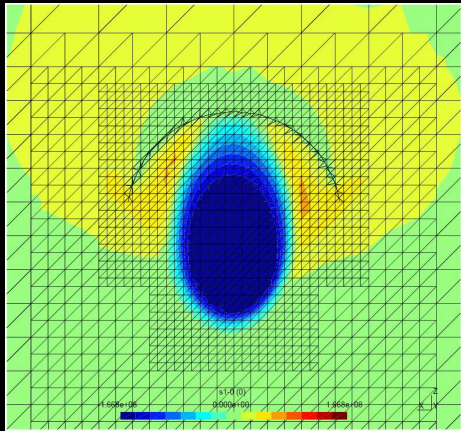
level	h (m)	Nb dofs	Nb iterations	time (s)
0	$2.5 \cdot 10^{-4}$	1344	528	0.59 s
1	$1.2 \cdot 10^{-4}$	2124	140	4.45 s
2	$6.2 \cdot 10^{-5}$	5262	75	1.61 s
3	$3.1 \cdot 10^{-5}$	13524	40	0.71 s
Nb dofs		22654	CPU time	7.4 s



$h_0/a \approx 1 \rightarrow$ enrichment at all levels







OUTLINE

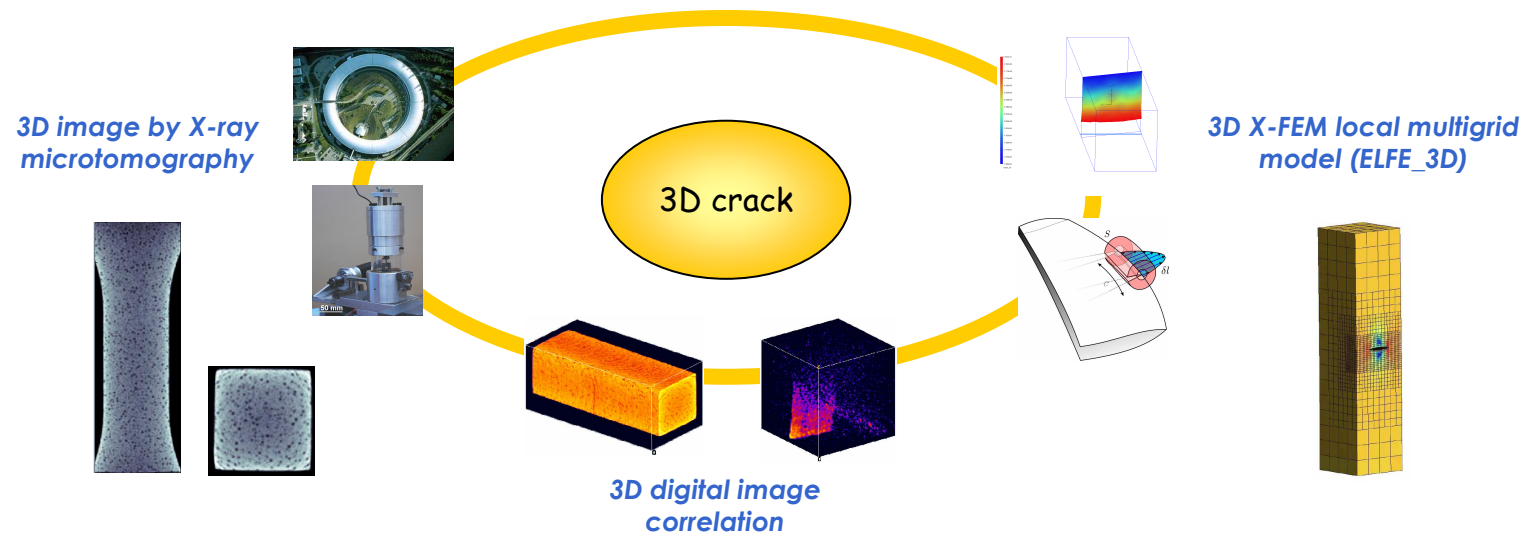
- 1 *Introduction of X-FEM+level sets for crack modeling*
- 2 *An example of multi-scale approach coupled with X-FEM*
- 3 **Conclusions & perspectives****

Main results

- *Accurate calculation of Stress Intensity factors for non-planar cracks (3D crack growth laws).*
- *One proposes a X-FEM local multi-grid strategy that ensures to capture in a unified approach different length scales which can occur in fracture mechanics.*
- *The crack is modeled on an independent local finite difference mesh adapted to the possible complexity of the crack shape during its propagation (+robust numerical integration of Hamilton Jacobi equations)*
- *Link between the convergence rate of the X-L-MG algorithm and the first enriched grid*
- *The introduction of local grids adapted to scale effects is not in contradiction with the non-remeshing property of the proposed method: indeed, the local grids are previously defined in the area of interest.*

Perspectives

- Automatic definition of local grids coupled with an adapted local error estimator
- Identification of 3D local crack growth law by the use of a X-FEM local multigrid strategy, 3D X-ray microtomography, and 3D digital image correlation (PROPAVANFIS Project, CETIM foundation, LMT / LaMCoS / MATEIS, France)



- Application to fretting, tribologic fatigue, extension to local nonlinear behaviors



Step 1 - Initialiser $\psi_I^* = w_I = 0$ pour chaque nœud du maillage

Step 2 - Boucle sur les éléments finis

Calculer les quantités

$$\nabla \psi = \sum_{J=1}^4 \nabla N_J \psi_J \quad \bar{V} = \int_E V dx$$

et les coefficients suivants pour chaque nœud I du tétraèdre considéré:

$$K_I = \bar{V} \frac{\nabla \psi \cdot \nabla N_I}{|\nabla \psi|} \quad \delta \psi = \sum_{J=1}^4 K_J \psi_J$$

$$\alpha_I = \frac{H\left(\frac{\delta \psi_I}{\delta \psi}\right)}{\sum_{K=1}^4 H\left(\frac{\delta \psi_K}{\delta \psi}\right)} \quad \text{avec} \quad \delta \psi_I = H(K_I) \left(\sum_{L=1}^4 H(K_L) \right)^{-1} \sum_{J=1}^4 H(-K_J) (\psi_J - \psi_I)$$

ou H est la fonction de Heaviside.

$$\psi_I^* = \psi_I^* + \alpha_I \delta \psi \quad (\nu \text{ est le volume de l'élément fini } E)$$

$$w_I = w_I + \alpha_I \nu$$

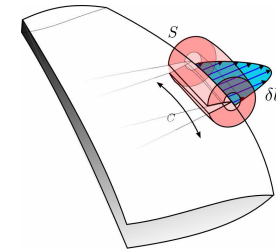
Step 3 - Boucle sur les nœuds du maillage pour l'intégration en temps

$$\begin{cases} \tilde{\psi}_I^{n+1} = \psi_I^n - \Delta t \frac{(\psi_I^*)^n}{w_I^n} \\ \psi_I^{n+1} = \frac{(\psi_I^n + \tilde{\psi}_I^{n+1})}{2} - \frac{\Delta t}{2} \frac{(\tilde{\psi}_I^*)^{n+1}}{\tilde{w}_I^{n+1}} \end{cases} \quad \text{[Barth and Sethian 1998]}$$

Stress Intensity Factors calculation

- Dissipated energy for a virtual crack extension

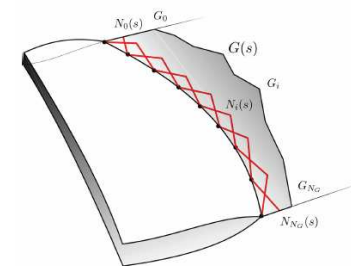
$$W_{diss} = \int_C \mathbf{G} \cdot \mathbf{s} \cdot \mathbf{n} \cdot \delta l \quad \mathbf{P} = \mathbf{W}_{diss} \cdot \mathbf{n} \cdot \delta l$$



- $G(s)$ is discretized along the front with curvilinear shape functions:

$$\mathbf{G}(s) = \sum_{i=1}^{N_G} \mathbf{G}_i(s) \mathbf{N}_i(s) \quad \mathbf{A}_{ij} = \int_C \mathbf{N}_i(s) \mathbf{N}_j(s) \cdot \mathbf{n} \cdot \delta l$$

[Parks et al., 2000]



- Diagonal matrix:

$$\mathbf{A}_{iijj} = \sum_{j=1}^{N_G} \mathbf{A}_{ij} = \int_C \sum_{j=1}^{N_G} \mathbf{N}_i(s) \mathbf{N}_j(s) \cdot \mathbf{n} \cdot \delta l = \int_C \mathbf{N}_i(s) \cdot \mathbf{n} \cdot \delta l$$

- Irwin formula

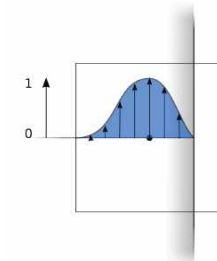
$$K = \sqrt{E' \left[\mathbf{G}(s) \right]} = \mu \cdot \mathbf{G}(s)$$

- Interaction integral

$$I_{int} = \int_V \mathbf{q}_{i,j} \left[\left(\frac{\partial u_{kl}^{aux}}{\partial x_{kl}} \right)_{ij} \left(\frac{\partial u_{kj}^{aux}}{\partial x_{ki}} - \frac{\partial u_{kj}^{aux}}{\partial x_{ki}} \right) \right]$$

- Contact, friction, plasticity, dynamics

$$J = \int_S \left(\frac{W}{p} \delta_{1j} - \sigma_{jk} u_{k,1} \right) \mathbf{q}_{1,j} \cdot \mathbf{n} \cdot dV - \int_{crack\ faces} \left(\frac{\partial u}{\partial x_1} \right) \cdot \mathbf{n} \cdot dV$$



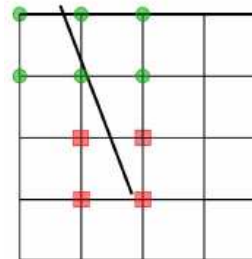
[Combesure, Suo, 1986] [Moës N., Gravouil A., Belytschko T., IJNME 2002]

[Gosz & al. 1997,2002, Béchet 2005, Réthoré 2005, Elguedj 2006, Ribeaucourt 2006]

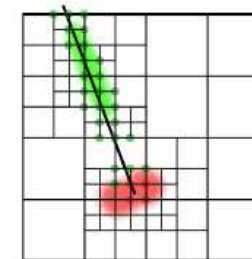
Un exemple de stratégie numérique multi-échelles

- ➔
X-FEM avec raffinement local du fait des non-linéarités
Éléments finis étendus multigrilles avec raffinement local pour la mécanique de la rupture
Algorithme multigrille localisé linéaire (MG-L-L) Full Approximation Scheme (FAS)

Problème linéaire modélisé avec X-FEM

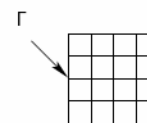


Problème non linéaire modélisé avec X-FEM

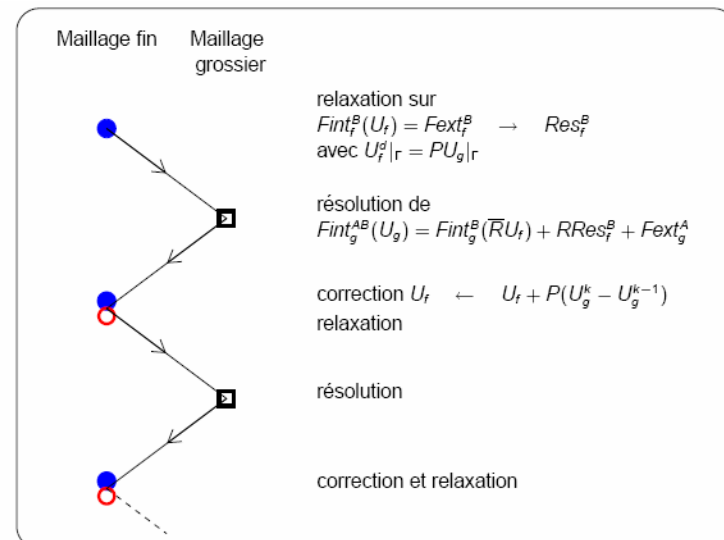
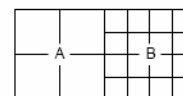


- Efficacité des solveurs itératifs pour la partie haute fréquence de la solution peu efficaces pour résoudre les composantes basses fréquences de la solution**

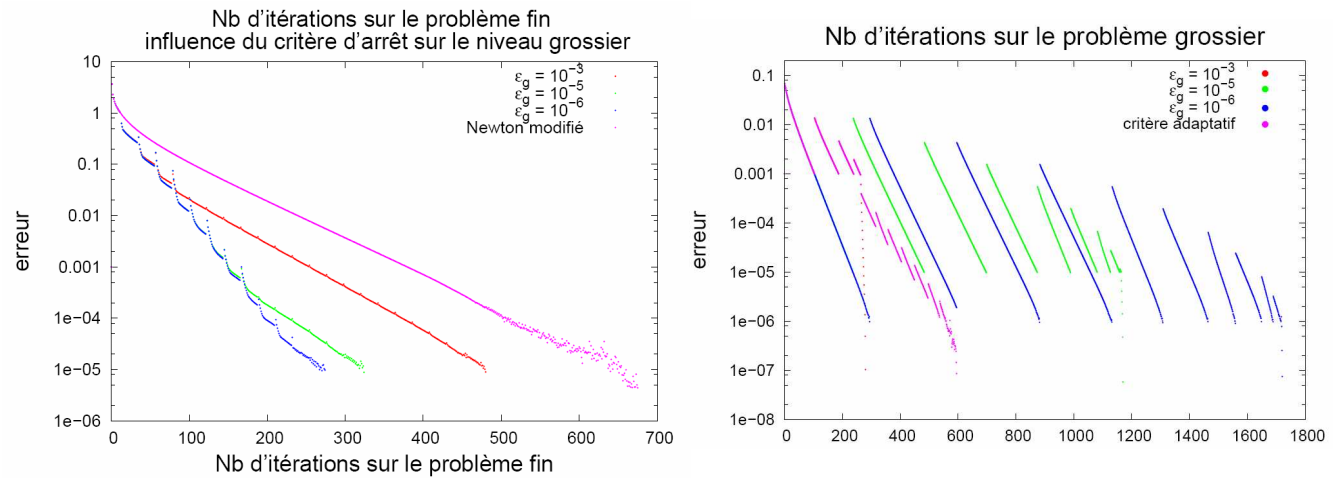
Chaque discrétisation est utilisée pour capturer une certaine gamme de fréquence en utilisant le solveur itératif de manière optimale



maillage cible



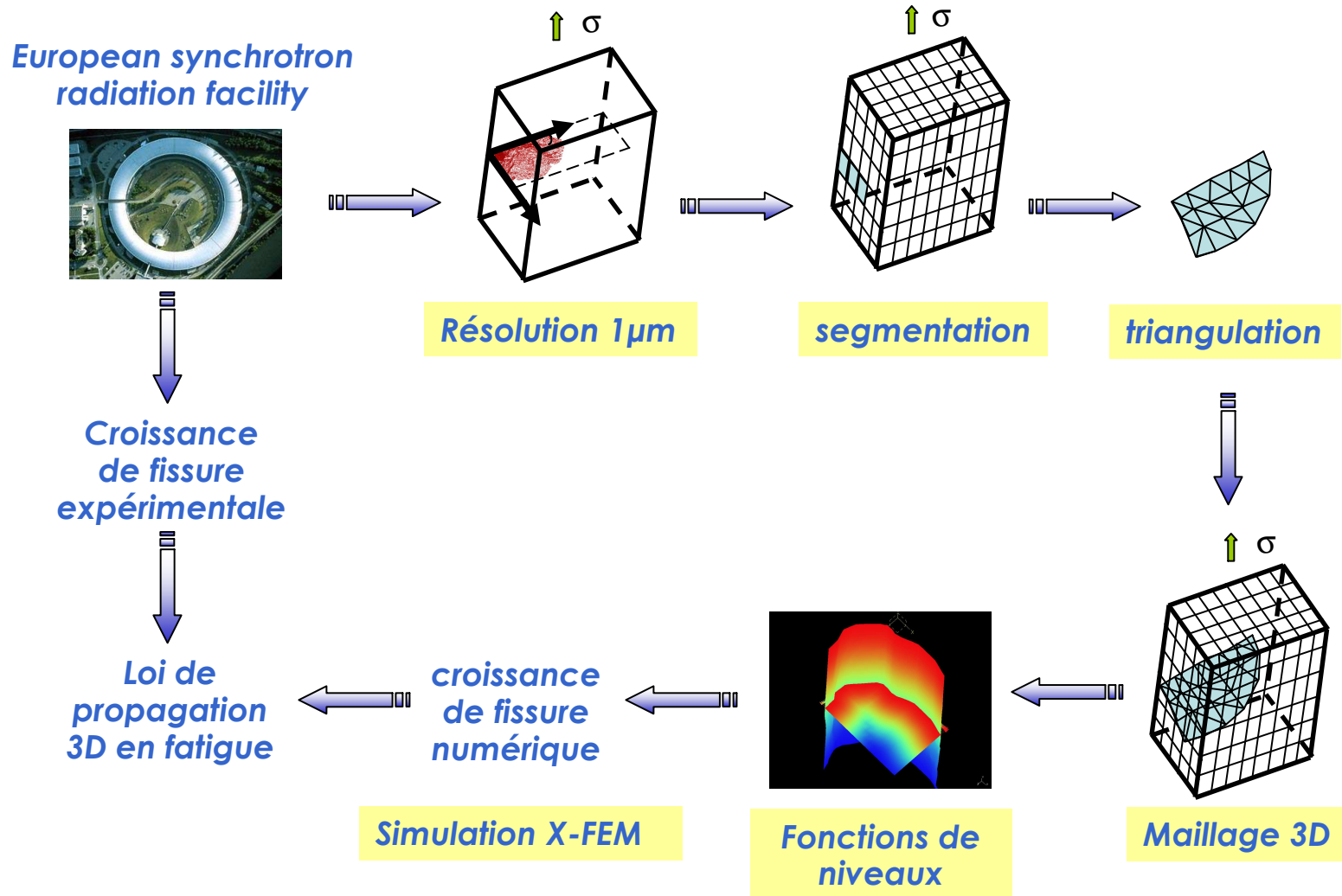
Exemple de stratégie numérique multi-échelles en non-linéaire



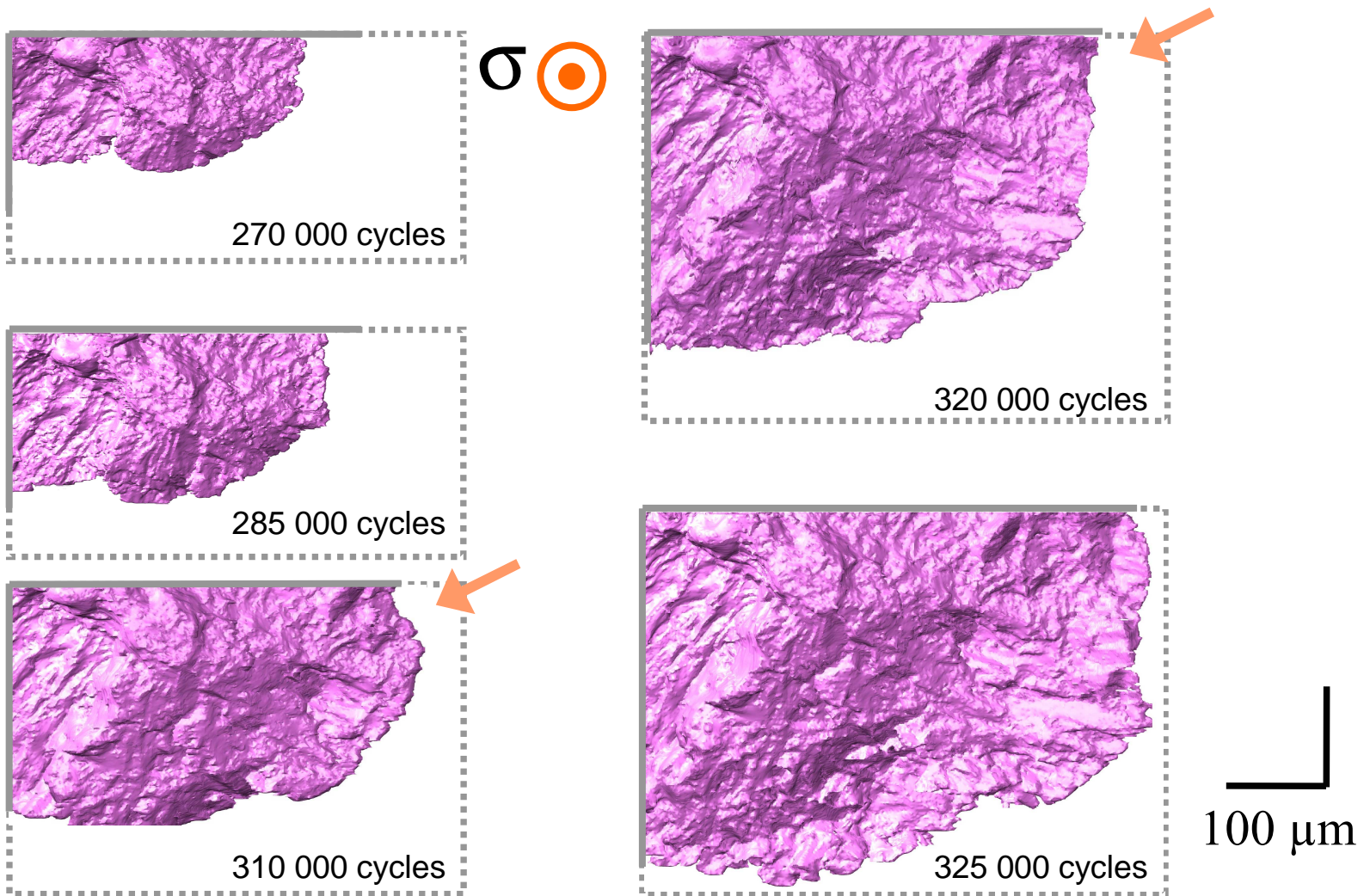
Critère d'arrêt sur le problème grossier

$$\varepsilon_g = \min(10^{-3}, C_f 10^{-2})$$

Vers un couplage entre l'imagerie tridimensionnelle et X-FEM



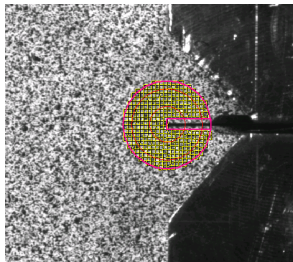
Microstructurally short cracks



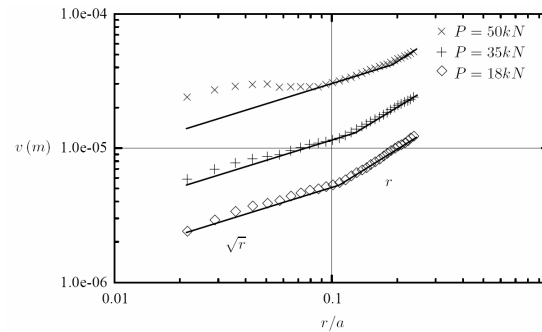
Fissuration en fatigue en mode mixte Plasticité confinée – effet de refermeture

- Mesure de champ par corrélation d'image (ICASOFT – MORESTIN F.)

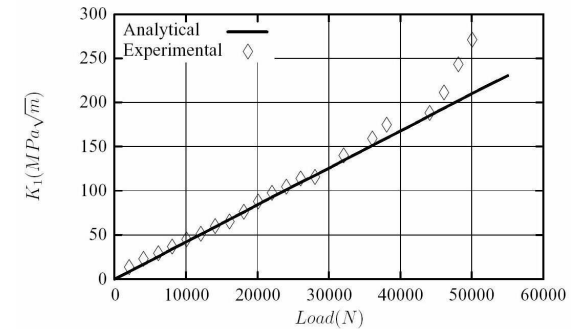
Résultats expérimentaux



Comportement asymptotique



FIC expérimentaux par techniques intégrales



[Réthoré J., Gravouil A., Morestin F., Combescure A., IJF, 2005]

- Base d'enrichissement en présence de plasticité confinée

$$\rightarrow \left\{ \begin{array}{l} r_1 \\ n \end{array} \right\} \left\{ \begin{array}{l} \sin_{\theta/2}, \cos_{\theta/2}, \sin_{\theta/2} \\ \sin_{\theta/2}, \cos_{\theta/2}, \sin_{\theta/2} \\ \sin_{\theta/2}, \cos_{\theta/2}, \sin_{\theta/2} \\ \sin_{3\theta/2}, \cos_{3\theta/2}, \sin_{3\theta/2} \end{array} \right\}$$

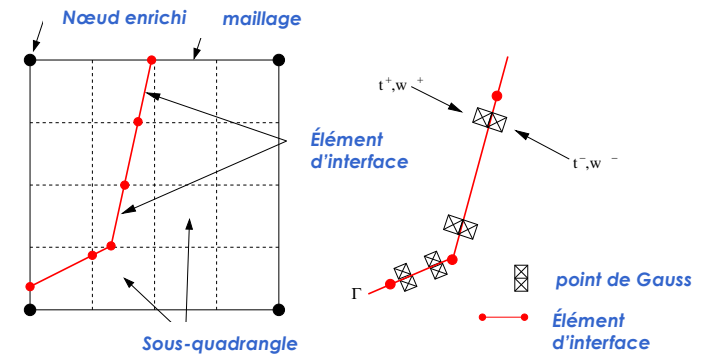
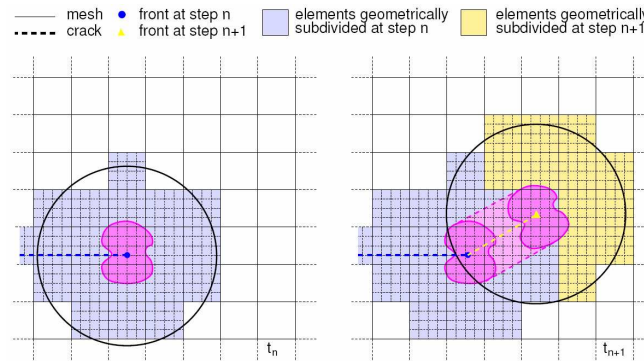
(lié à l'écroissage du modèle élasto-plastique)

[Elguedj T., Gravouil A., Combescure A., CMAME, 2006]

Fissuration en fatigue en mode mixte Plasticité confinée – effet de refermeture

- **Stratégie de propagation de fissure en fatigue à 2 échelles (pas de remaillage ni de projection de champ)**

$$R_{sub} = \beta \times \frac{\pi}{16}$$



- **Modélisation du contact et du frottement**

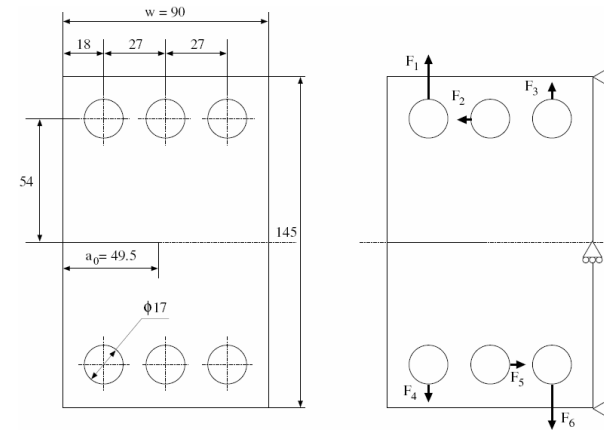
$$\begin{aligned} \Rightarrow \int_{\Omega} \bar{\sigma}_n^i \cdot \bar{\sigma}_n^i \, d\Omega &= \int_{\partial_2 \Omega} \bar{\sigma}_n^i \cdot \bar{\sigma}_n^i \, dS + \int_{\Gamma} \bar{\sigma}_n^i \cdot \bar{\sigma}_n^i \, dS + \int_{\Gamma} \bar{\sigma}_n^i \cdot \bar{\sigma}_n^i \, dS \\ &+ \int_{\Gamma} \left(\bar{\sigma}_n^i + \alpha w_{i-1} \right) \cdot \bar{\sigma}_n^i \, dS - \int_{\Gamma} \left(\bar{\sigma}_n^i + \alpha w_i \right) \cdot \bar{\sigma}_n^i \, dS \end{aligned}$$

[Elguedj T., Gravouil A., Combescure A., IJNME, 2007]

Fissuration en fatigue en mode mixte Plasticité confinée – effet de refermeture

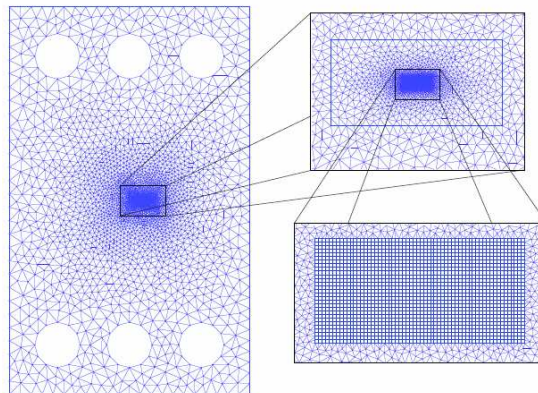
- **Éprouvette CTS: effet de surcharge**

L'éprouvette est soumise à une croissance de fissure totale de $\Delta a = 0.5$ mm (20 pas pour FEM, 2 pas pour X-FEM), puis soumise à une surcharge de rapport 2.5 puis une croissance totale de $\Delta a = 0.5$ mm

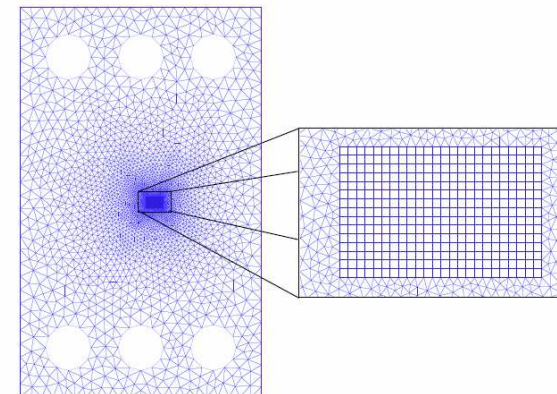


- **Comparaison FEM / X-FEM**

Maillage FEM

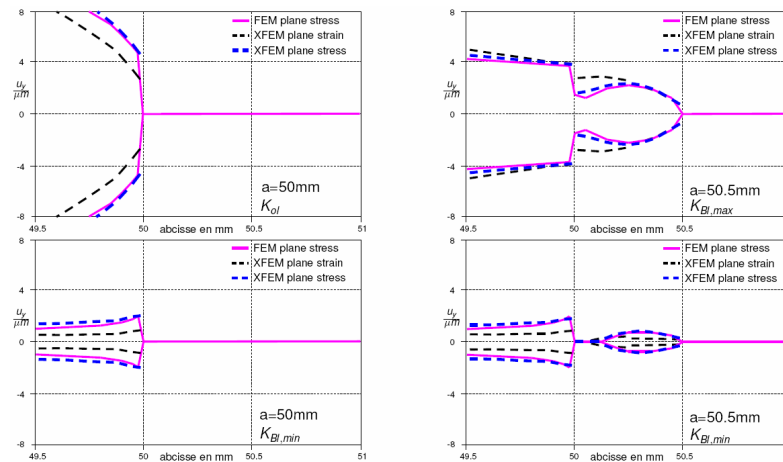


Maillage X-FEM (10 fois plus grossier)

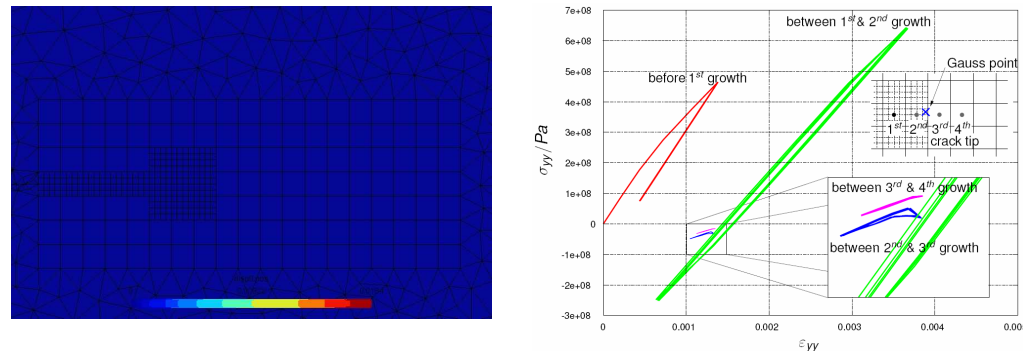


Fissuration en fatigue en mode mixte Plasticité confinée – effet de refermeture

- Comparaison du déplacement vertical au niveau des faces de la fissures entre les résultats de FEM et X-FEM

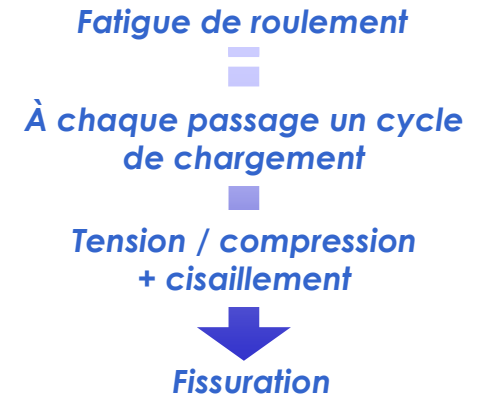
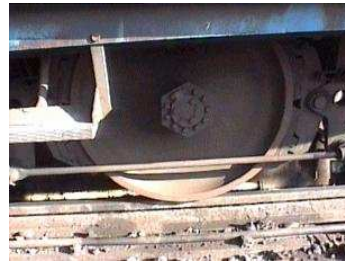


- Croissance de fissure dans une éprouvette CT sollicitée en mode I

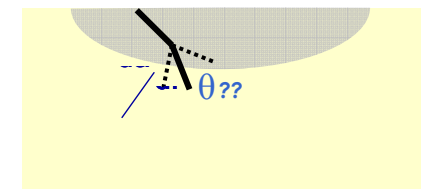
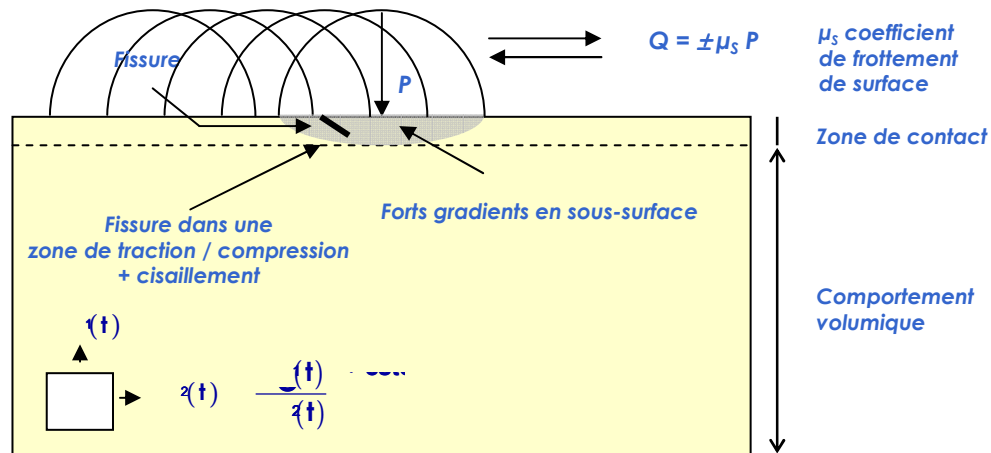


Fatigue de roulement

● Etude du contact roue-rail



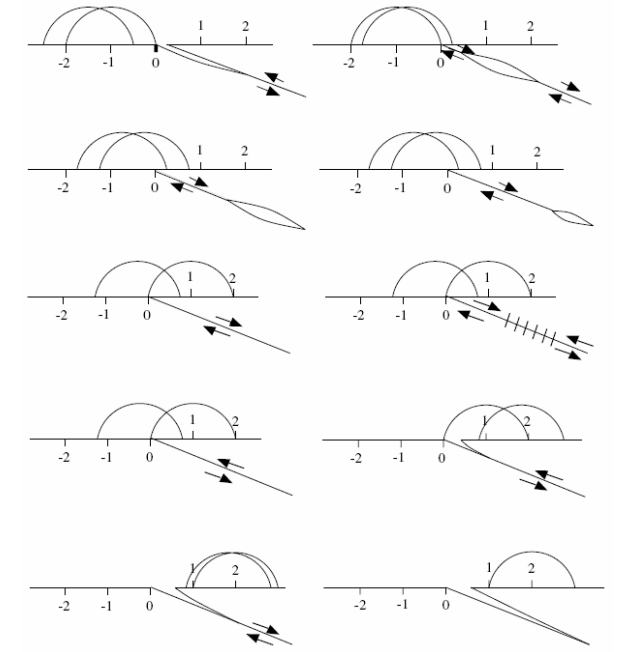
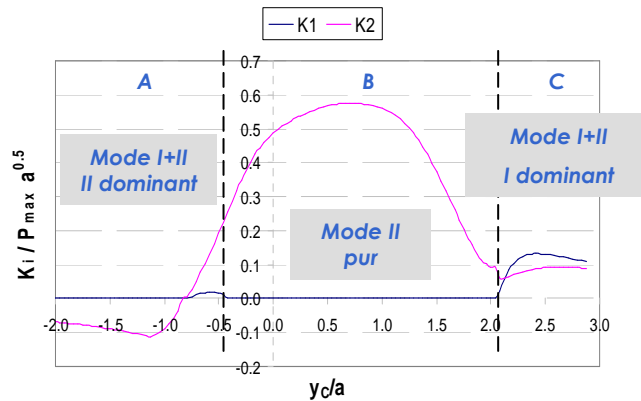
● Modèle numérique bi-dimensionnel



Le comportement de la fissure dépend fortement de sa longueur comparée à la zone de fort gradient

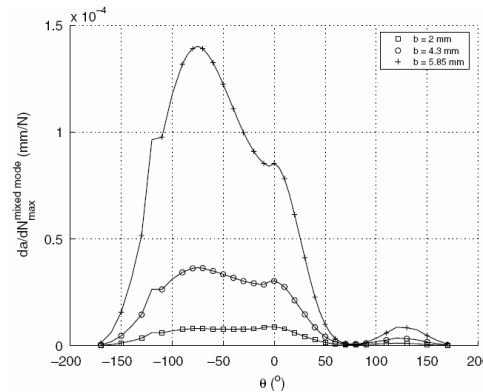
Fatigue de roulement

- Formulation quasi-statique incrémentale X-FEM (méthode LATIN) (indicateur d'erreur normal et tangentiel découplé)

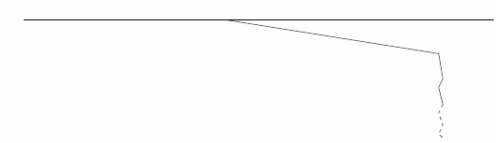


- Critère en fatigue de contact à la fin d'un cycle de chargement

(on considère les quantités maximales pendant 1 cycle)



$$= 2.0 \cdot 10^9 \left(\frac{\Delta k_1}{1_{max}} + 0.772 \frac{\Delta k_2}{2_{max}} \right)$$



[Dolbow J., Moës N., IJNME, 2002] [Ribeaucourt, Baietto, Gravouil, CMAME, 2007]

[Hourlier & al. 1982] [Amestoy 1983] [Lamacq V., Baietto M.C., Vincent L., Tribol. Int., 1997]